minerals

MDPI

Article

Geochemical Fingerprinting of Conflict Minerals Using Handheld XRF: An Example for Coltan, Cassiterite, and Wolframite Ores from Democratic Republic of the Congo, Africa

Alireza K. Somarin

Department of Geology, Brandon University, Brandon, MB R7A 6A9, Canada; somarina@brandonu.ca

Received: 18 July 2019; Accepted: 16 September 2019; Published: 18 September 2019

Abstract: Conflict minerals are those mined in politically unstable regions of the world and are then sold to finance war or other illegal activities. Industrial manufacturers are required to show that minerals used in their applications are not derived from conflict areas. Several geochemical and geochronological methods have been suggested to fingerprint conflict minerals; however, all these methods require sophisticated and extensive laboratory procedures. Portable X-ray fluorescence data of 108 samples from various location in Democratic Republic of the Congo shows that cassiterite and wolframite ores from all studied regions can be fingerprinted using various discrimination diagrams. Coltan ore samples from several regions can also be discriminated using major and trace elements of these samples. In addition, patterns in chondrite-normalized spider diagrams for each region are unique and can be used as fingerprinting tools.

Keywords: coltan; conflict minerals; columbite; tantalite; cassiterite; wolframite; portable XRF

1. Introduction

Conflict minerals have always been an attractive topic, not only from a scientific point of view but also from political, international, and industrial views; these minerals can be used to fund war or illegal activities. Importantly, the end-user industries need to document the source of these minerals. In the 1990's, the popular saleable item were so-called "blood diamonds," with monies financing wars in some regions in Africa. Diamonds were easy to carry and smuggle, but this trade has been severely curtailed with the introduction of United Nations Security Council resolution 1173 that prohibited diamond sales from conflict regions (e.g., Angola) without a certificate of origin. Other illegally-traded materials have now become popular, such as cassiterite, wolframite, and coltan (tin, tungsten and niobium/tantalum ores) due to the widespread use of these metals in consumer electronics, medical devices, and military applications. Much of the illicit mining of these materials occurs in the eastern portion of the Democratic Republic of Congo (DCR).

With the advent of U.S. Securities and Exchange Commission (SEC) Conflict Minerals Law (sometimes called the 3TG rule), manufacturers have to submit a Conflict Minerals report every year for those conflict minerals used in their manufacturing process that document the supply chain trail. There has been a push back onto primary smelters to confirm that the ores they are using have come from a reputable source and are not part of the conflict mineral trade. This is done both through Certified Trading Chains (CTC) as well as determining an analytical fingerprint that provides a distinctive geochemical, geochronological [1], and mineralogical signature of individual production sites using multiple laboratory methods. All these methods require sophisticated and extensive sample preparation and laboratory analytical procedures. For example, the German Federal Agency for Geosciences and Natural Resources (BGR) developed a comprehensive method that requires a

complete analysis of sample by several techniques including whole rock X-ray florescence (XRF), X-ray diffractometry (XRD), inductively coupled plasma mass spectrometry (ICP-MS), inductively coupled plasma optical emission spectrometry (ICP-OES), electron microprobe, U-Pb dating, and laser ablation inductively coupled plasma mass spectrometry (LA-ICPMS) [1].

Field-portable X-ray florescence (FPXRF), as handheld or benchtop portable analyzers, is a technique that has been used in various fields from geology/mineralogy to mining (green-field exploration to exploitation and ore grade control), environmental science, metallurgy, geo-archeology, and even oil/gas exploration and production [2–11]. Expansion of application of these instruments in many fields is mainly due to speed (fast, real time analysis), high sample density (high number of analyses), relatively inexpensive analyses, and ease of use in the field or remote labs. They offer a low-cost solution to rapidly determine the chemistry of materials, which could be used to determine the provenance of any given ore with region-specific element markers, or combinations of elements ("fingerprints"). This paper examines the use of HHXRF in delineating geochemical features of columbite, tantalite, cassiterite and wolframite ores from various regions of DRC.

Deposit Types

Niobium, Ta, Sn, and W are high field strength elements (HFSE) that are generally incompatible in silicate phases during magmatic differentiation, and as a result, are enriched in late-stage magmas where they have the potential to create economic ore deposits. Tantalum and Nb are commonly associated with three types of igneous rocks (Figure 1, Table 1) [12,13]: (1) carbonatites and associated rocks; (2) alkaline to peralkaline granites and syenites; and (3) granites and pegmatites enriched in Li, Cs and Ta (LCT granite family) [2]. In addition, placer deposits of these metals can form due to weathering, transportation, and deposition in a sedimentary environment. Generally, these secondary deposits occur relatively close to their primary source.

There are two main types of primary deposits in DRC:

1. Carbonatite-sourced secondary deposits: A good example of this type deposit is Lueshe Nb deposit, in the northeast DRC (Figure 2). This deposit is related to a Cambrian syenite-carbonatite intrusion with a core of syenite (~800 m in diameter), which is rimmed by a ring dyke of calcite carbonatite and dolomite carbonatite. This complex has experienced an intense weathering and supergene alteration, which resulted in the accumulation of weather-resistant pyrochlore $(Na,Ca)_2Nb_2O_6(OH,F)$ in the lateritic profile. This accumulation is accompanied by chemical transformations without any change in the mineralogical state [14].
2. Pegmatites and quartz veins: Granite-related Ta-Nb-Sn-W mineralization is associated with pegmatites and quartz veins in the Kibara (the Katanga region of the DRC) and Karagwe–Ankole (part of eastern DRC, Burundi, Rwanda, Uganda) belts (Figure 2) [15–18]. Four generations of granites (G1 to G4) have been identified [17]: G1-3 intruded at 1380 ±10 Ma in the Palaeo- and Meso-proterozoic rocks of the Kibara belt followed by intrusion of the youngest granite, G4, at ~986 Ma, which was intruded by pegmatite at ~960 Ma. Some of these pegmatites have coltan mineralization. Quartz-tin mineralization occurred at ~940 Ma and its associated hydrothermal activity altered pegmatites intensely [17]. Columbite, tantalite and local cassiterite and wolframite are mined both from deeply weathered pegmatites and from secondary placer deposits derived from the pegmatites.

The secondary deposits formed from these two types of mineralization should have distinct geochemical fingerprints as ore mineralogy in these deposits varies significantly. Carbonatite-sourced secondary deposits can be recognized by high Nb and possibly high REE concentrations and low Ta, Sn and W concentrations, whereas pegmatite-related placer deposits would have lower REE and higher Ta, Sn and W.

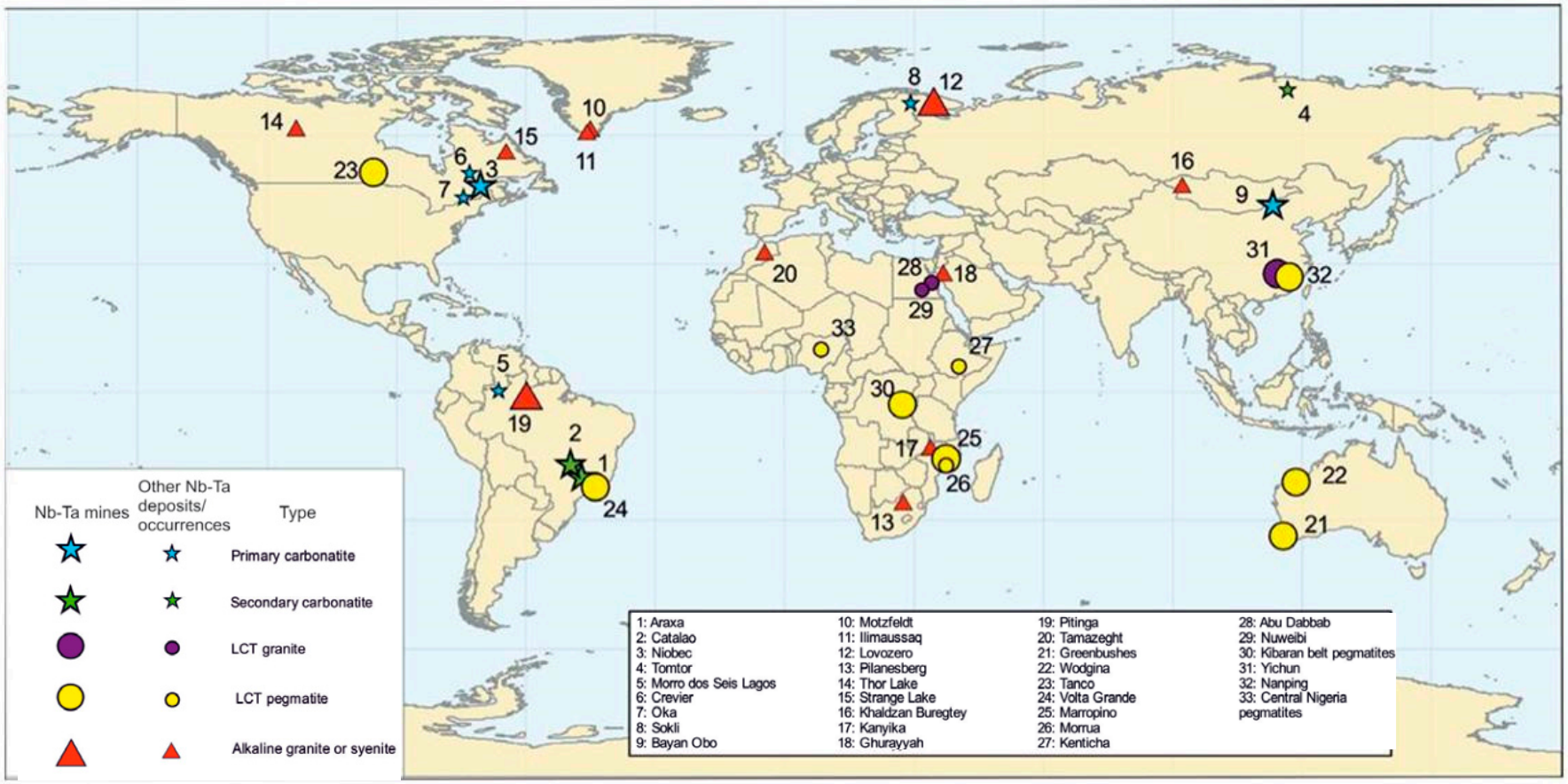

Figure 1. Distribution of various types of Nb-Ta deposits worldwide [13].

Table 1. Common types of Ta-Nb deposits with a brief description, grade, tonnage, and examples [13].

Type	Brief Description	Typical Grades and Tonnage	Major Examples
Carbonatite-hosted primary deposits	Niobium deposits found within carbonatite in alkaline igneous provinces.	Niobec, proven & probable reserves: 23.5 million tonnes at 0.59% Nb_2O_5	Niobec, Canada; Oka, Canada
Carbonatite-sourced secondary deposits	Zones of intense weathering or sedimentary successions above carbonatite intrusions in which Nb ore minerals are concentrated.	<1000 million tonnes at up to 3% Nb_2O_5 in lateritic deposits. Up to 12% Nb_2O_5 in placer deposit at Tomtor. Tonnage not known.	Araxa and Catalao, Brazil; Tomtor, Russia; Lueshe, Democratic Republic of Congo
Alkaline granite and syenite	Nb and lesser Ta deposits associated with silicic alkaline igneous rocks. Ore minerals may be concentrated by magmatic or hydrothermal processes.	Generally < 100 million tonnes at grades of 0.1 to 1% Nb_2O_5 and < 0.1% Ta_2O_5	Motzfeldt and Ilimaussaq, Greenland; Lovozero, Russia; Thor Lake and Strange Lake, Canada; Pitinga, Brazil; Ghurayyah, Saudi Arabia; Kanyika, Malawi
LCT-type granite	Ta and lesser Nb deposits associated with peraluminous leucogranitic plutons, which are often hydrothermally altered.	Generally < 100 million tonnes, at grades of < 0.05% Ta_2O_5	Abu Dabbab and Nuweibi, Egypt; Yichun, China
LCT-type pegmatite	Ta and lesser Nb deposits associated with pegmatites of LCT (Li-Cs-Ta-enriched) type	Generally < 100 million tonnes, at grades of < 0.05% Ta_2O_5	Greenbushes and Wodgina, Australia; Tanco, Canada; Volta Grande, Brazil; Kenticha, Ethiopia; Morrua & Marropino, Mozambique

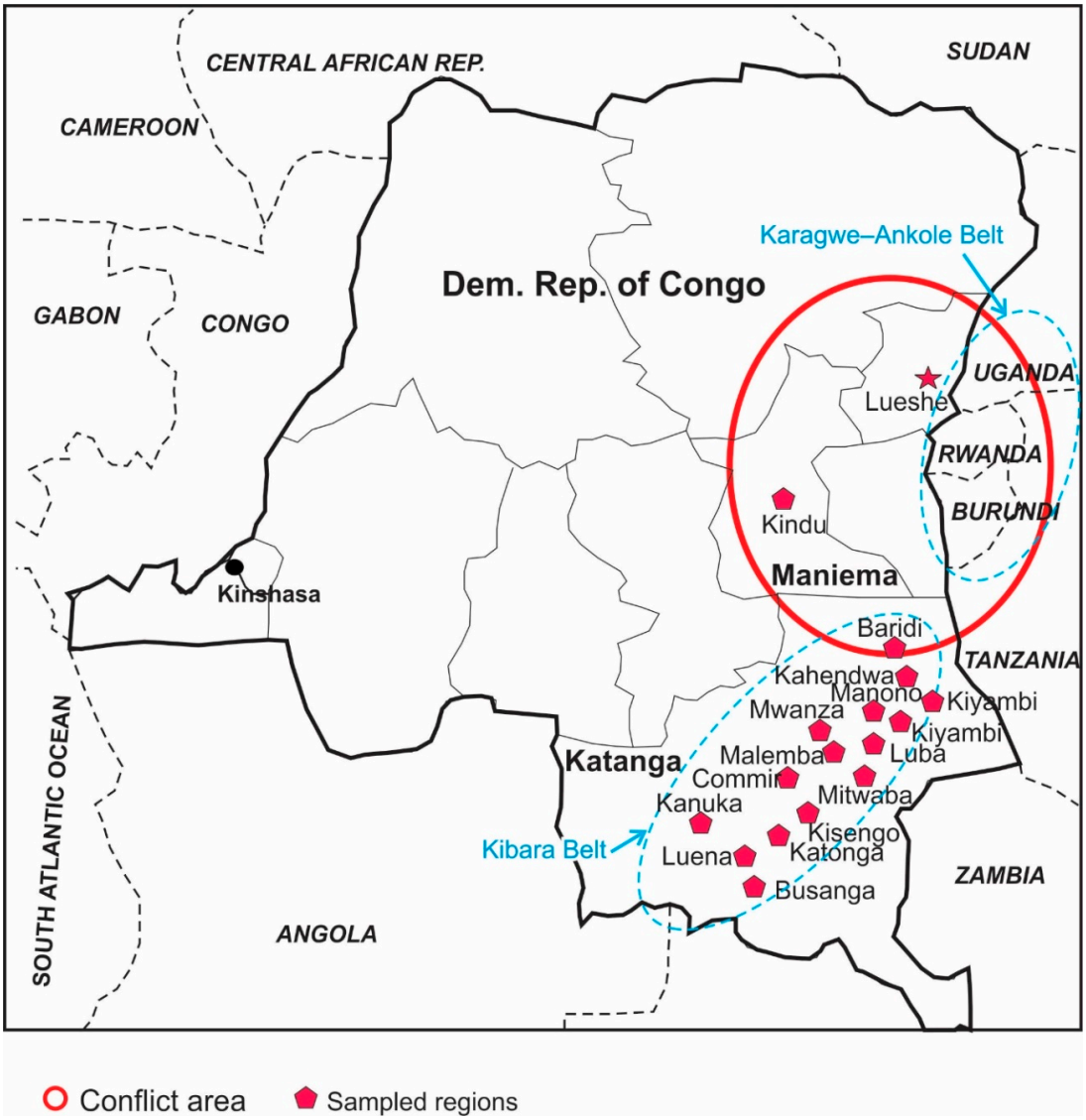

Figure 2. Location of regions in two provinces (Maniema, Katanga) that were sampled for this study. Lueshe Nb deposit in NE side, as well as Kibara and Karagwe-Ankole metalogenic belts (oval dash lines), are also shown.

2. Materials and Methods

A series of 99 fine-grained and 8 coarse-grained placer ore specimens were sampled from 15 sites in the DRC using panning and sieving methods, including 10 wolframite ore (from Katonga, Luena and Manono regions), 49 coltan ore (from Baridi, Kahendwa, Kanuka, Katonga, Kisengo, Kiyambi, Luba, Luena, Malemba, Manono, and Mwanza regions), and 48 tin samples (46 samples from Busanga, Commir, Kanuka, Luena, Malemba, Manono, Mitwaba, and Mwanza deposits and 2 samples from the Kindu region in the Maniema Province) (Table 2).

Each sample is not pure wolframite, columbite-tantalite or cassiterite minerals, rather, they may contain several minerals in each ore type (e.g., various Ta-Nb minerals in the coltan ore). The collected samples represent the true variations in mineralogy across different parts of the same deposit. These samples represent true ore that is traded in the mineral market of DRC.

Sub-samples were collected via handpicking using optical binoculars. All samples were pulverized to smaller than 200 mesh and packed into standard 32 mm cups fitted with 4 μm polypropylene film. At time of cupping, each sample was measured with the Thermo RadEye to determine radioactivity of material as some of the samples contain U and Th.

Table 2. Samples used in the study. Locations are shown in Figure 2.

Ore Type	# of Samples	Location	Province
Wolframite	4	Katonga	Katanga
	1	Manono	Katanga
	5	Luena	Katanga
Cassiterite	6	Busanga	Katanga
	6	Commir	Katanga
	6	Kanuka	Katanga
	6	Luena	Katanga
	6	Malemba	Katanga
	6	Manono	Katanga
	6	Mitwaba	Katanga
	4	Mwanza	Katanga
	2	Kindu	Maniema
Coltan	5	Baridi	Katanga
	6	Kahendwa	Katanga
	5	Kanuka	Katanga
	4	Katonga	Katanga
	6	Kisengo	Katanga
	3	Kiyambi	Katanga
	4	Luba	Katanga
	4	Luena	Katanga
	4	Malemba	Katanga
	5	Manono	Katanga
	3	Mwanza	Katanga

A series of certified reference materials, as well as the sampled specimens, were analyzed using a handheld ThermoFisher Niton XL3t-GOLDD (Figure 3) using Mining Mode so that spectra could be obtained in all 4 filters: Main, Low, High, Light (30 s analysis time in each filter). This mode uses fundamental parameters and relies on the detector's response to pure element spectra. The factory calibration uses these spectra to identify the elements present in each sample and to calculate peak intensities from spectrum and showing results after applying corrections. The built-in TaHf calibration program was determined to be the most suitable method as it provides simultaneous analysis of suite of elements (Table 3), including the vital elements for discrimination purposes. This is a factory built-in special mode designed for coltan and associated minerals; in this mode, the performance of the analyzer is enhanced by eliminating elements with X-ray energies close to Nb and Ta. The energy values (in kilo electron volt, Kev) for Kα, Kβ, Lα, and Lβ lines are respectively 16.61, 18.62, 2.17, 2.26 for Nb and 57.52, 65.21, 8.15, 9.34 for Ta.

Factory calibration can produce reliable data for some elements (particularly base metals) in some rock/soil matrices; however, the analytical accuracy and precision can be low mainly due to peak overlap or matrix difference between the analyzed unknown sample and factory calibration samples. User calibration (i.e., calibration made by user) utilizing known samples (e.g., certified standards) was employed to verify FPXRF data quality. In order to increase the accuracy of the analytical data, the analyzer was calibrated for all the required elements and the analytical performance was checked against 35 certified reference materials (Table 3). All the specimens were analyzed twice, and a third analysis was carried out in cases where significant discrepancies existed between the previous analyses. Limits of detection for the elements of interest ranges from 3 ppm for trace elements to 3500 ppm for major elements (Table 3). Elements with potential spectral overlap (such as REE) or with values close to detection limit (1.5 times the detection limit) were not used during this study. Portable XRF is mostly a partial analysis technique that provides assay results for selected elements of interest. As a result, some elements may be missing and therefore the total of analyzed elements may not be 100%.

Figure 3. Analysis of coltan ore samples by HHXRF showing a real time qualitative test by the user.

Table 3. List of elements provided by the handheld analyzer. Limits of detection (LOD in ppm), as well as certified standards used for the calibration of the handheld analyzer, are included.

Elem.	LOD	Elem.	LOD	Certified Standard		Certified Standard	
U	5	Rb	3	SiO2	Blank	OREAS 142	Sn ore
Th	4	Se	10	BH-1	W ore	BCS355	Sn ore
Bi	3	As	3	CT-1	W ore	FQZ X1808	Nb ore
Pb	5	Zn	8	DH-1a	U-Th ore	NCSDC35008	Sn ore
W	35	Cu	12	DL-1a	U-Th ore	NCSDC35009	Sn ore
Ta	5	Ni	25	MP-1	Zn-Sn-Cu-Pb ore	NCSDC35011	Sn ore
Nd	90	Co	20	MP-1b	Zn-Sn-Cu-Pb ore	NCSDC35012	Sn ore
Ce	60	Fe	35	OKA-1	Nb mineral	NCSDC70006	Mo ore
La	50	Mn	55	TAN-1	Ta ore	NCSDC73309	Stream sediment
Ba	35	Cr	20	DH SX18-01	Nb ore	NCSDC86315	Ta ore
Cs	30	V	10	DH SX18-04	Nb ore	NCS DC86306	Ta ore
Sb	12	Ti	10	AMIS0019	Sn porphyry	HK3453A	Ta-Nb
Sn	13	Ca	50	AMIS0020	Sn porphyry	HK3462	Ta-Nb
Cd	8	K	40	AMIS0021	Sn porphyry	HK3541	Ta-Nb
Ag	10	S	70	IGS26	Sn-W ore	HK3574	Ta-Nb
Mo	3	P	200	IGS34	Tantalite		
Nb	3	Si	500	OREAS 98	Cu ore		
Zr	3	Al	500	OREAS 99b	Cu-Ag ore		
Y	5	Mg	3500	OREAS 140	Sn ore		
Sr	3			OREAS 141	Sn ore		

3. Results

The tin ore samples from the eight different regions in the Katanga Province, DRC, range from 40 to 63% Sn, with 157 to 10,415 ppm Nb, <3 to 17,657 ppm Ta, and <3 to 19,320 ppm W (Table 4). Most of these samples are radioactive with up to 89 ppm U and 436 ppm Th. Visual examination of cassiterite ore specimens indicates that some regions have darker color samples. This may be partially related to their high Fe and Ti content [19]. The wolframite ore samples contain 36 to 51% W, 674 to 113,783 ppm Sn, 1249 to 2819 ppm Nb, and <3 ppm Ta (Table 5). Up to 1362 ppm Th was found in one sample from Katonga. In the coltan samples, Ta and Nb concentrations range from 9.5 to 30% and 2.6 to 36%, respectively (Table 6). Tungsten was detected only in 3 samples: from Katonga (47,250 ppm), Luena (83,688 ppm), and Malemba (3029 ppm). All samples contain Sn from 0.2 to 24%. Most samples are radioactive with Th and U ranging from 515 to 6427 ppm and 108 to 1368 ppm, respectively. Samples from Luba and Katonga do not contain Th.

Table 4. Chemical analysis of cassiterite ore samples (in ppm). Nd, La, Ba were not detected. _Not detected.

Sample	Location	Sn	Nb	Ta	W	Ce	Th	Zr	Y	Sr	U	Rb	Mn	K	P	Fe	Ti
bsng-01	Busanga	603,579	212	_	_	_	_	87	17	_	16	_	1316	1195	_	29,176	1077
bsng-02		605,984	181	_	_	_	_	88	9	_	_	5	615	1032	_	24,706	1458
bsng-03		599,768	225	_	_	_	_	93	_	_	_	_	898	992	_	21,725	1444
bsng-04		633,612	177	_	_	_	_	85	_	_	_	5	366	597	_	16,425	1375
bsng-05		616,379	214	_	_	_	_	110	9	_	_	_	1852	692	_	19,693	1338
bsng sn07		595,287	157	_	_	_	_	106	_	_	_	9	1116	1878	_	40,880	1644
cmr01	Commir	563,890	465	1585	_	_	_	129	18	_	_	45	_	4927	_	28,271	2814
cmr02		557,392	465	1341	_	_	_	126	17	_	_	45	355	5057	_	33,730	3191
cmr03		545,369	332	748	_	_	_	116	20	_	_	37	337	4125	_	43,248	4028
cmr04		543,514	382	1215	281	_	_	113	15	11	_	40	436	5277	_	40,398	2908
cmr05		539,881	633	1242	_	_	_	118	9	8	_	42	389	5653	_	35,108	2851
cmr sn06		466,834	316	753	_	_	_	118	21	7	_	40	848	6186	_	81,021	4596
knk sn01	Kanuka	493,129	10,415	17,657	_	_	172	3318	314	_	89	17	9185	4105	_	10,522	6369
knk sn02		515,889	8303	14,966	_	_	145	3895	184	_	48	14	5829	2585	_	7248	3581
knk sn03		508,808	5604	12,468	_	_	148	3807	175	_	82	18	3601	2645	_	5122	2559
knk sn04		493,366	5198	11,913	_	_	127	4098	166	9	77	12	2957	3087	_	5618	2440
knk sn05		499,326	3467	10,330	_	_	172	4620	155	_	84	18	1517	3687	_	4341	2772
knk sn06		422,513	1536	6585	_	_	222	12,548	98	_	51	28	_	7427	_	5122	5288
ln sn01	Luena	561,085	1577	1354	17,201	985	359	600	212	11	16	21	5300	3078	3699	21,549	1628
ln sn02		572,068	2391	1934	14,005	_	420	580	273	9	28	12	5211	1447	4398	19,201	1869
ln sn03		562,250	1915	1731	18,997	_	436	386	306	12	30	13	5856	2093	1089	26,819	1055
ln sn04		591,226	1792	1297	7592	_	232	373	86	13	_	14	4283	1360	_	18,274	1512
ln sn05		587,664	1422	1174	6177	_	370	290	163	_	_	16	3433	2137	_	19,116	1060
ln sn07		549,024	1012	1356	3890	_	141	3309	59	13	_	26	3441	4516	_	41,232	2677
mlb sn01	Malemba	496,026	1754	1765	_	_	269	921	265	10	18	27	1054	3173	_	28,844	6421
mlb sn02		466,756	1447	2002	_	_	158	660	175	_	23	21	1457	2679	_	27,666	5278
mlb sn03		490,270	2413	2416	_	_	252	1061	235	6	_	25	1795	2303	_	29,500	10,214
mlb sn04		509,202	1519	2220	467	_	205	990	151	9	_	41	952	3286	_	27,140	5049
mlb sn05		531,744	1310	2093	_	_	174	780	89	_	15	20	390	1991	_	17,975	2947
mlb sn07		402,722	664	1134	_	_	86	2550	88	_	13	36	498	3189	_	31,592	2763

Table 4. *Cont.*

Sample	Location	Sn	Nb	Ta	W	Ce	Th	Zr	Y	Sr	U	Rb	Mn	K	P	Fe	Ti
mnn sn01	Manono	471,080	2697	6378	_	_	107	3848	32	_	38	11	1363	1301	_	6602	2529
mnn sn02		465,172	2619	6524	_	_	_	3574	12	_	30	10	880	1351	_	6242	1697
mnn sn03		560,713	3150	8131	_	_	81	3927	28	_	26	18	1500	1422	_	7433	2702
mnn sn04		554,214	2940	8116	_	_	_	3678	30	_	44	11	1159	958	_	7448	2807
mnn sn05		556,193	2817	8157	_	_	92	7293	40	_	39	16	944	550	_	5418	4806
mnn sn 05		450,275	1891	5860	_	_	173	9170	80	_	72	29	1965	2048	_	11,357	9185
mtb 01	Mitwaba	512,959	1008	1335	5984	_	54	374	68	6	_	8	2084	1815	_	49,215	28,435
mtb 02		520,706	898	657	348	741	271	993	262	_	16	10	850	1831	_	41,743	25,323
mtb 03		523,738	735	509	338	895	231	599	181	_	24	9	858	2072	_	41,576	17,218
mtb 04		536,930	517	430	_	_	120	340	134	_	_	13	898	2631	_	38,149	13,009
mtb 05		515,917	666	448	_	_	158	423	176	_	_	11	693	2081	_	39,316	21,480
mtb sn07		425,956	377	363	_	1784	158	355	735	9	17	33	541	4990	_	43,921	16,771
mnzw 01	Mwanza	518,377	1488	3627	_	_	179	607	184	6	27	41	1435	3282	_	22,871	3060
mnzw 02		532,493	1703	3580	_	_	164	381	128	7	17	35	1111	2975	_	26,738	2944
mnzw 06		578,705	1163	2713	_	_	101	255	48	_	_	26	572	2258	_	13,453	2220
mwnz sn06		471,932	762	2594	_	_	91	922	32	16	_	79	522	5740	_	30,282	3633
sa2	Kindu	509,567	1136	1922	3674	714	324	1580	133	_	19	12	1512	2044	_	45,061	13,591
klo		556,390	1433	1092	19,320	_	406	722	90	7	17	25	5671	2715	3976	22,764	6436

Table 5. Chemical analysis of wolframite ore samples (in ppm). Ta was not detected. —Not detected.

Sample	Location	Sn	Nb	W	Nd	Ce	La	Ba	Th	Zr	Y	Sr	U	Rb	Mn	K	P	Fe	Ti
ktng w08	Katonga	1863	1249	487,618	1606	1647	1060	174	773	246	102	_	_	_	6913	370	46,103	126,606	1163
ktng w09		9833	1386	442,865	1599	1969	1314	_	909	480	138	_	43	_	7930	549	39,936	138,035	6107
ktng w10		674	1298	480,265	1698	1960	1167	251	868	284	109	_	41	8	6762	_	45,446	130,805	1291
ktng w11		7930	2352	421,252	2354	2935	1947	402	1362	701	212	6	58	_	9978	939	136,213	152,175	10,451
mnn w02	Manono	7155	2819	507,004	735	174	_	183	69	31	160	13	26	_	25,357	_	49,309	95,633	_
ln w01	Luena	110,375	1805	378,093	692	208	382	_	_	45	67	10	_	9	65,090	1560	31,353	53,283	1308
ln w02		113,783	2296	388,223	655	_	_	_	95	39	30	22	_	10	69,446	1194	33,666	56,043	_
ln w03		102,407	1911	368,425	536	371	329	295	_	27	41	28	_	11	66,489	2378	31,872	80,184	696
ln w04		69,731	2324	414,509	849	383	463	329	_	70	91	40	_	11	60,201	1566	35,991	89,085	735
ln w06		79,615	2424	400,803	674	177	_	248	_	36	49	40	18	12	72,188	1586	34,847	78,563	791

Table 6. Chemical analysis of coltan ore samples (in ppm). _Not detected.

Sample	Location	Sn	Nb	Ta	W	Nd	Ce	La	Ba	Th	Zr	Y	Sr	U	Rb	Mn	K	P	Fe	Ti
tmk13	Baridi	4569	26,256	197,175	_	526	149	_	604	572	1069	19	43	108	30	16,583	2801	3526	99,700	6183
tmk14		24,135	39,842	257,858	_	486	_	_	812	515	720	34	18	177	15	20,299	2280	4442	110,508	4503
tmk15		4842	49,526	279,696	_	417	227	_	278	800	1209	32	25	197	20	21,510	2371	5752	93,954	6831
tmk16		2874	37,981	230,759	_	633	295	_	303	669	1128	38	33	119	34	16,545	2316	3826	96,267	7500
tmk17		2047	32,964	222,229	_	378	122	_	429	547	932	32	50	126	20	16,427	1950	5503	95,509	6152
tmk 07	Kahendwa	41,971	151,734	255,140	_	1593	1580	1196	1357	960	1559	857	_	311	15	64,122	1076	8423	98,807	22,171
tmk 08		11,667	259,013	174,237	_	1118	707	_	2084	_	977	224	_	426	_	65,250	2154	_	102,251	15,619
tmk 09		63,223	216,909	156,625	_	1407	1725	1128	548	_	895	269	_	171	_	53,242	2217	6856	110,388	26,193
tmk 10		50,897	197,724	115,541	_	1518	2209	1723	359	689	940	653	_	226	_	42,865	3768	_	98,725	27,025
tmk 11		8694	318,647	167,390	_	_	_	_	_	_	1187	_	_	128	_	56,895	1252	9319	109,618	2172
tmk 12		20,307	279,824	199,619	_	1254	428	_	621	_	1499	_	_	181	_	57,221	1669	_	102,090	3789
knk cl01	Kanuka	106,596	147,119	190,025	_	1511	884	718	460	894	1419	480	_	777	_	83,324	1806	8397	40,182	7522
knk cl02		58,933	97,201	97,776	_	1489	1464	802	279	1418	5603	2451	_	226	15	99,357	1436	12,018	126,586	115,270
knk cl03		53,425	126,487	131,947	_	2160	2468	1490	247	2166	7834	3118	_	242	24	107,247	776	18,163	90,768	76,631
knk cl04		44,567	116,207	123,262	_	1503	1916	968	_	1872	7404	3784	_	240	20	102,280	1070	18,957	106,265	87,947
knk cl05		79,986	85,449	95,856	_	2474	3396	1769	_	1890	9505	3070	28	274	16	77,719	1831	14,808	102,376	75,782

Table 6. *Cont.*

Sample	Location	Sn	Nb	Ta	W	Nd	Ce	La	Ba	Th	Zr	Y	Sr	U	Rb	Mn	K	P	Fe	Ti
ktng cl06	Katonga	98,486	99,326	288,880	_	896	453	_	725	598	1507	_	54	462	30	73,927	2167	8081	41,603	3178
ktng cl07		73,567	82,731	265,064	47,250	968	696	326	546	858	1715	60	43	436	42	66,811	3207	26,358	64,889	5572
ktng cl08		93,378	89,190	298,845	_	1258	680	439	822	953	1856	31	40	357	85	68,831	3609	5548	39,839	5387
ktng cl11		169,444	100,413	231,559	_	1103	755	770	909	722	1337	26	44	389	66	66,492	3044	5790	44,405	8163
tmk 01	Kisengo	41,366	61,871	219,011	_	_	480	_	324	_	2366	94	28	314	18	37,725	2856	6981	93,829	8917
tmk 02		41,149	61,567	219,143	_	1118	673	319	763	_	1868	112	20	255	_	37,885	2375	6778	98,495	6255
tmk 03		40,159	65,982	233,385	_	1044	745	455	796	_	2129	788	21	289	28	36,614	3501	6867	93,668	8134
tmk 04		34,146	56,162	201,436	_	505	362	_	765	_	2317	116	23	232	20	34,510	3312	5549	97,645	8449
tmk 05		40,265	59,723	202,301	_	705	638	436	799	_	2141	205	24	267	_	33,502	2772	3664	100,116	8159
tmk 06		45,547	54,120	189,079	_	715	890	403	727	_	2330	293	33	259	16	31,419	2849	5057	105,903	11,548
kymb-cl-08	Kiyambi	101,583	152,887	244,793	_	1435	502	_	478	1579	1240	_	122	506	36	49,592	3360	10,249	95,203	3841
kymb-cl-09		128,958	104,915	214,978	_	1354	642	669	1126	740	1694	157	37	546	32	55,585	3302	6721	80,224	7040
kymb-cl-12		113,026	151,377	211,363	_	667	457	_	437	1172	2325	85	28	774	50	59,413	4107	9060	79,396	5905
tmk 18	Luba	76,347	108,203	241,173	_	742	485	_	1156	_	1250	_	_	575	_	63,059	2294	6407	73,084	3717
tmk 19		68,640	86,011	233,447	_	1126	310	320	853	_	1355	_	17	473	_	59,113	3399	5651	55,261	3894
tmk 20		67,319	104,638	227,126	_	_	_	_	643	_	1394	31	22	395	_	60,061	2282	_	62,500	2058
tmk 21		103,902	72,604	218,669	_	1279	551	622	474	_	1200	188	_	386	_	65,079	2043	5768	54,663	5953
ln cl01	Luena	39,075	362,518	144,023	_	2171	1924	773	742	3225	1305	880	_	1115	27	73,904	1282	_	13,4599	14,056
ln cl02		77,066	199,214	164,974	83,689	1423	915	752	286	1748	1202	747	_	842	_	84,021	1582	37,958	72,865	4979
ln cl04		240,108	138,372	159,187	_	2203	1975	1428	674	1774	920	604	_	507	22	61,906	1717	8287	63,880	6825
ln cl05		46,364	235,442	203,212	_	1617	1895	628	719	2052	1193	1056	25	1112	_	74,650	1064	10,817	94,241	12,178
mlb cl07	Malemba	14,752	186,169	208,856	_	1175	616	_	302	1749	1989	525	_	967	25	87,873	1875	10,093	58,981	9609
mlb cl08		107,035	302,419	171,660	3029	_	1015	1090	532	2956	1526	305	49	677	41	66,719	_	_	97,234	4888
mlb cl12		96,334	217,000	190,939	_	11,731	21,007	12,853	_	6427	816	10,785	_	1368	_	69,842	_	49,949	84,843	6562
mlb cl01		20,121	201,768	235,466	_	921	689	453	_	1226	927	580	_	1061	_	98,587	1925	13,755	44,083	6717
mnn cl01	Manono	41,302	137,238	193,925	_	1521	1089	758	2162	1208	2814	539	17	323	38	87,006	2097	8688	96,478	18,144
mnn cl02		57,856	133,020	181,996	_	1393	811	355	1844	1407	3601	593	25	333	23	82,411	1866	_	107,490	17,924
mnn cl03		43,041	162,592	216,369	_	1314	1194	662	1686	1127	2948	599	_	412	21	93,726	2293	8865	73,721	15,981
mnn cl04		83,504	145,254	200,455	_	1351	1260	837	1515	739	3167	590	_	538	_	85,684	2344	8126	63,291	13,265
mnn cl05		37,026	168,489	216,717	_	1336	970	609	1197	586	2468	590	_	443	_	89,805	1779	9363	69,813	13,049
mwnz cl08	Mwanza	40,005	266,340	241,071	_	1008	375	_	607	2806	4089	198	75	925	30	94,988	1059	9657	66,774	4186
mwnz cl10		40,369	238,972	235,377	_	995	1027	_	_	2257	1152	681	_	934	21	96,481	1407	8733	61,949	10,150
mwnz cl04		33,684	163,981	205,803	_	1419	1116	333	242	956	2495	591	_	860	_	91,188	1282	11,269	50,629	8535

4. Discussion

Conflict minerals and their derivative metals (Ta, Na, Sn, W) are an integral part of many electronics and technology industries. According to many national and international laws, these industries are committed to responsible sourcing of these minerals to safeguard human rights and to use only conflict-free minerals, i.e., minerals that do not directly or indirectly benefit or finance armed groups in DRC or adjoining countries. As a result, discrimination of conflict minerals from conflict-free ones is an important task from industrial and social perspectives. Several analytical and laboratory methods have been proposed and tested to identify provenance of these minerals [1,20–22].

Geochemical composition of the analyzed samples (Tables 4–6) shows that some regions have specific elemental characteristics that reflect their unique mineralogy. Combination of these characteristics as single elements, ratios, or composite factors, can be used to discriminate various regions of ore types.

4.1. Fingerprinting Cassiterite Ore

The following discrimination diagrams are used to differentiate cassiterite ore from various regions.

Sn-W-(Ta + Nb) ternary diagram: In many deposits, particularly pegmatite deposits, Sn may be associated with W, Nb, and Ta. On this basis, these elements are used to discriminate some of the deposits. In order to spread out data from various regions, the Sn-W-(Ta + Nb) ternary diagram is constructed using these factors: Sn/10, 20 W, and 20 (Nb + Ta) (Figure 4). Based on this diagram, the regions within the DRC are classified as follows:

(1) Sn-rich region: Busanga
(2) Ta + Nb-rich regions: Manono, Kanuka
(3) W-rich regions: Luena, Kindu
(4) Sn and Ta + Nb-rich regions: Commir, Malemba, Mwanza

Cassiterite ore samples from the Mitwaba region show a wide range of W and Ta + Nb.

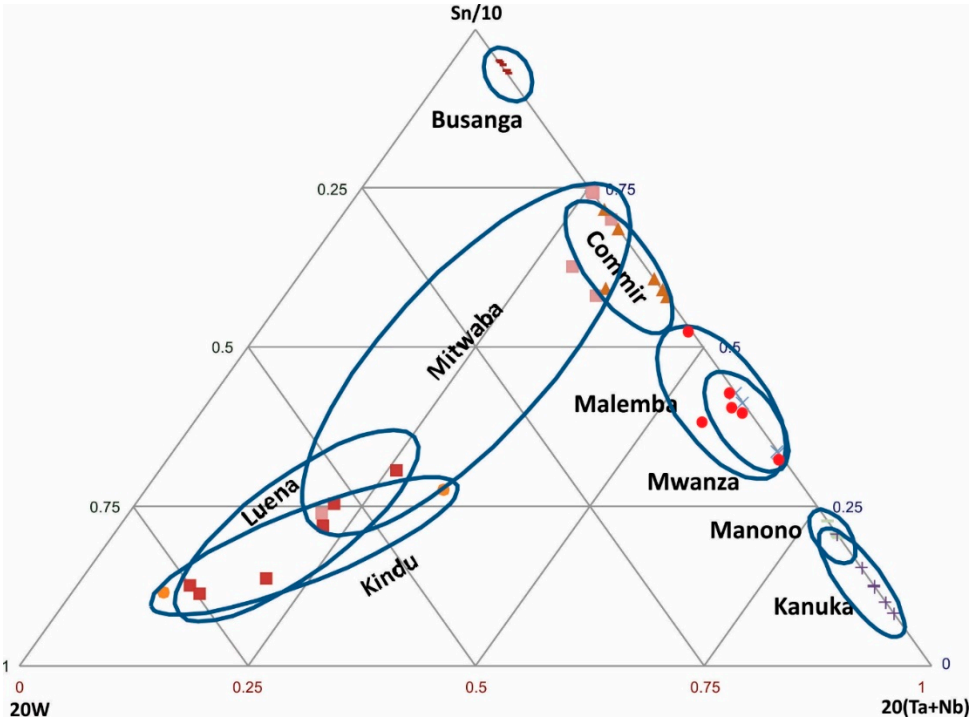

Figure 4. Discrimination of cassiterite samples from various regions based on Sn-W-(Ta + Nb).

Sn vs. (Fe/Ti) diagram: Cassiterite ore from several regions can be discriminated using Sn vs. 100 (Fe/Ti) diagram (Figure 5a). Malemba, Mwanza, Commir, Luena, and Busanga cassiterite ore samples plot in discrete parts of this diagram, whereas rest of the regions (Kindu, Mitwaba, Kanuka, Manono) do not show considerable variation in Fe/Ti ratio by increasing Sn content.

Ti vs. (Ti/Nb + Ta) diagram: This diagram discriminates Mitwaba and Busanga tin ore from other regions (Figure 5b).

W + Th vs. Fe/Ti diagram: This diagram discriminates Luena cassiterite ore samples (Figure 5c).

Y + Th vs. Nb + Ta diagram: This diagram distinguishes Busanga, Commir, Manono and Kanuka cassiterite ore samples (Figure 5d).

W + Th vs. Ti/(Ta + Nb) diagram: This diagram differentiates Mitwaba, Kindu and Luena cassiterite ore samples (Figure 5e).

Ta/Nb vs. Ti/(Ta + Nb) diagram: This diagram discriminates Busanga, Mitwaba, Malemba and Mwanza tin ore samples (Figure 5f).

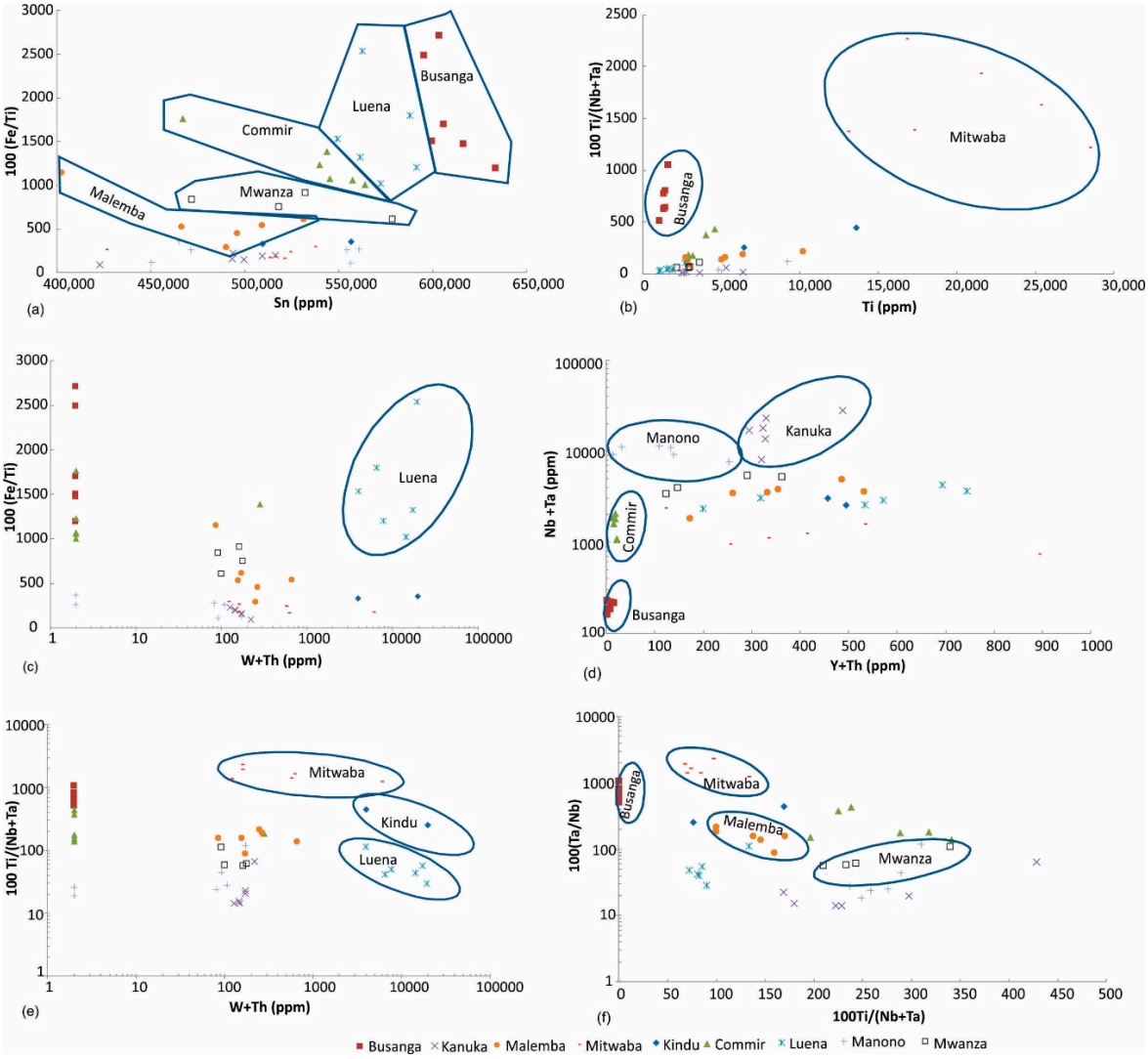

Figure 5. Discrimination of (**a**) Malemba, Mwanza, Commir, Luena, and Busanga, (**b**) Mitwaba and Busanga, (**c**) Luena, (**d**) Busanga, Commir, Manono, and Kanuka, (**e**) Mitwaba, Kindu, and Luena, (**f**) Busanga, Mitwaba, Malemba, and Mwanza cassiterite ore samples.

4.2. Fingerprinting Wolframite Ore

The following discrimination diagrams are constructed to fingerprint these wolframite ore samples.

W-Sn-(Ta + Nb) ternary diagram: Tungsten may occur with Sn, Nb, and Ta in pegmatite deposits. In addition, W may occur in quartz veins and mix with Nb-Ta or Sn during weathering of primary deposits (i.e., placer formation processes). The W-Sn-(Ta + Nb) discrimination diagram is used to evaluate this possible association (Figure 6). Wolframite ore samples from all three regions have very low Ta + Nb. Samples from Katonga and Manono are similar and have low Sn concentrations, whereas Luena samples have the highest Sn concentration amongst the analyzed samples.

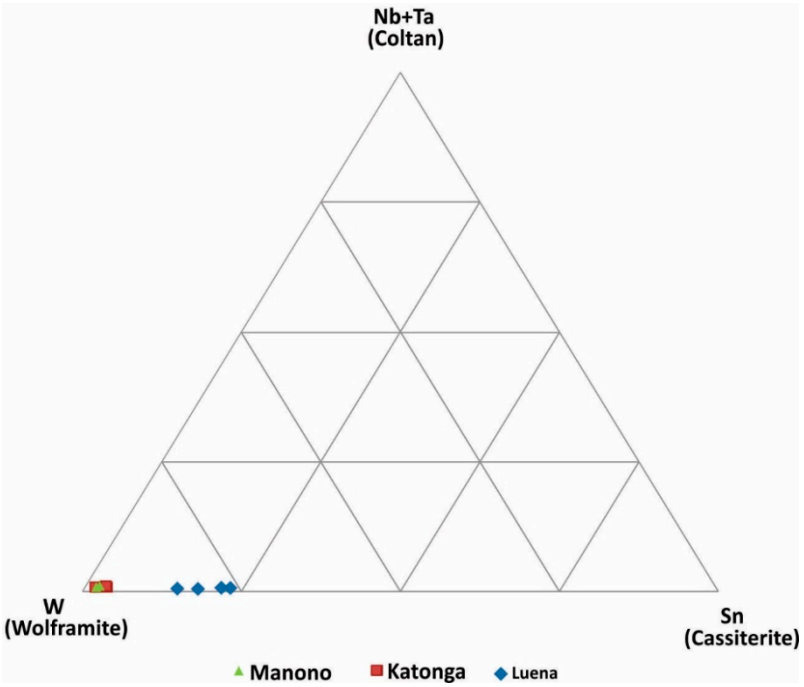

Figure 6. Discrimination of wolframite ore samples based on W, Sn and Nb+Ta concentrations.

W-Fe-Mn ternary diagram: This diagram (Figure 7) is used to discriminate various wolframite ore samples because natural wolframite grains are composed of three main metals: Fe, Mn, and W. Katonga and Luena wolframite ore samples are characterized by high Fe and high Mn, respectively. Only one sample from Manono was analyzed and it may not be a representative of this region.

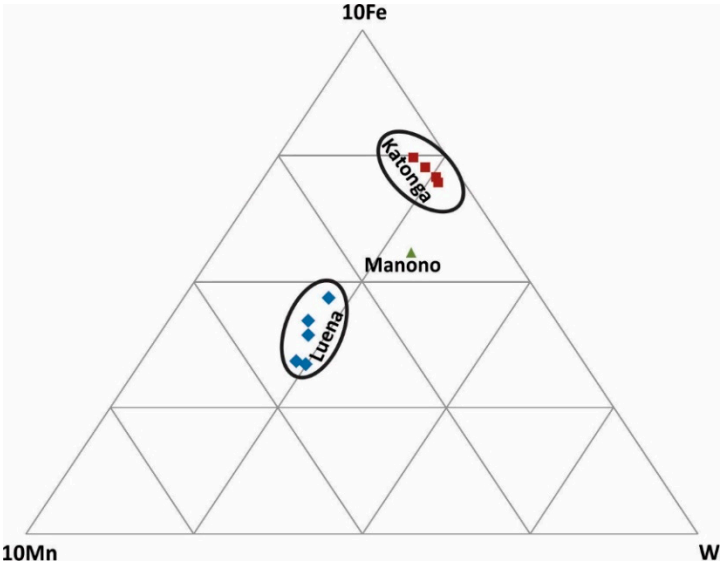

Figure 7. Discrimination of wolframite ore samples based on Fe, Mn, and W concentrations.

Fe vs. Mn diagram: Based on the above-mentioned criteria, Fe-Mn diagram can clearly discriminate wolframite ore from these three regions (Figure 8a).

Other diagrams: Other trace elements that can occur in the late-stage pegmatite deposits and may show variation in the analyzed wolframite ore samples include Sn, Th, and Zr. Combinations of different discrimination diagrams (Figure 8b–f) can be used to successfully differentiate wolframite ore from these three regions.

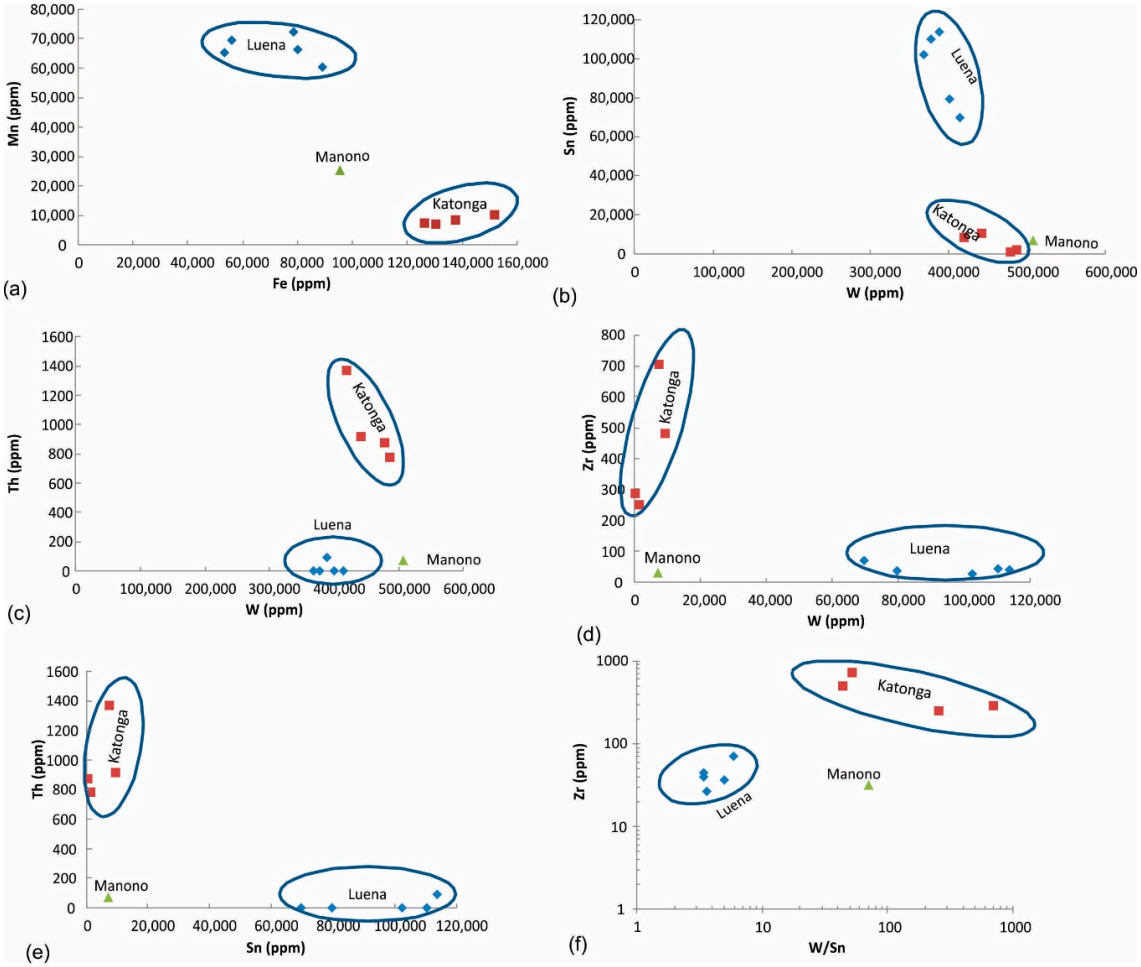

Figure 8. Discrimination of wolframite ore samples based on (**a**) Fe and Mn, (**b**–**f**) combination of W, Sn, Th, and Zr concentrations.

4.3. Fingerprinting Coltan Ore

Nb vs. Ta diagram: Nb and Ta are the main economic metals of coltan ore, and the concentrations of these elements can be used to discriminate the sampled regions (Figure 9a). This diagram can differentiate Baridi and Kisengo coltan ore samples, which have the lowest Nb concentrations. Most of Kanuka samples plot on the low Nb-low Ta part of the diagram. Katonga samples are characterized by ~10% Nb and >23% Ta.

100 (Nb/Ta) vs. Sn diagram: Tin is commonly associated with coltan and can be used as a discriminator (Figure 9b). Coltan ore samples from Baridi, Kisengo, Manono, and Kanuka plot in discrete areas in this diagram. Most samples from Kahendwa have high Nb/Ta ratio. Katonga, Luba and Kiyambi samples are characterized by high Sn and 100 Nb/Ta of ~50. Samples from other regions show overlap.

Mn vs. Fe/Mn diagram: Iron and Mn are two major elements of coltan minerals; however, their concentrations and relative abundances may vary significantly depending on the geology of the area. The Mn vs. Fe/Mn diagram (Figure 9c) can be used to fingerprint coltan ore samples from Baridi,

Kisengo and Kahendwa/Kiyambi regions. Samples from Kahendwa and Kiyambi plot in the same area in this diagram. Coltan from the remaining regions have low Fe/Mn ratios, which cannot be used to discriminate them.

Mn vs. Fe/Ti diagram: Titanium may substitute for Nb and Ta in the structure of coltan minerals. In addition, Ti can accompany these minerals as its own discrete minerals such as rutile (TiO_2). The Mn vs. Fe/Ti diagram (Figure 9d) can be used to fingerprint coltan ore samples from Baridi, Kisengo and Kanuka regions. One Kanuka sample plots with Manono samples, and it is likely that it has been mis-labeled.

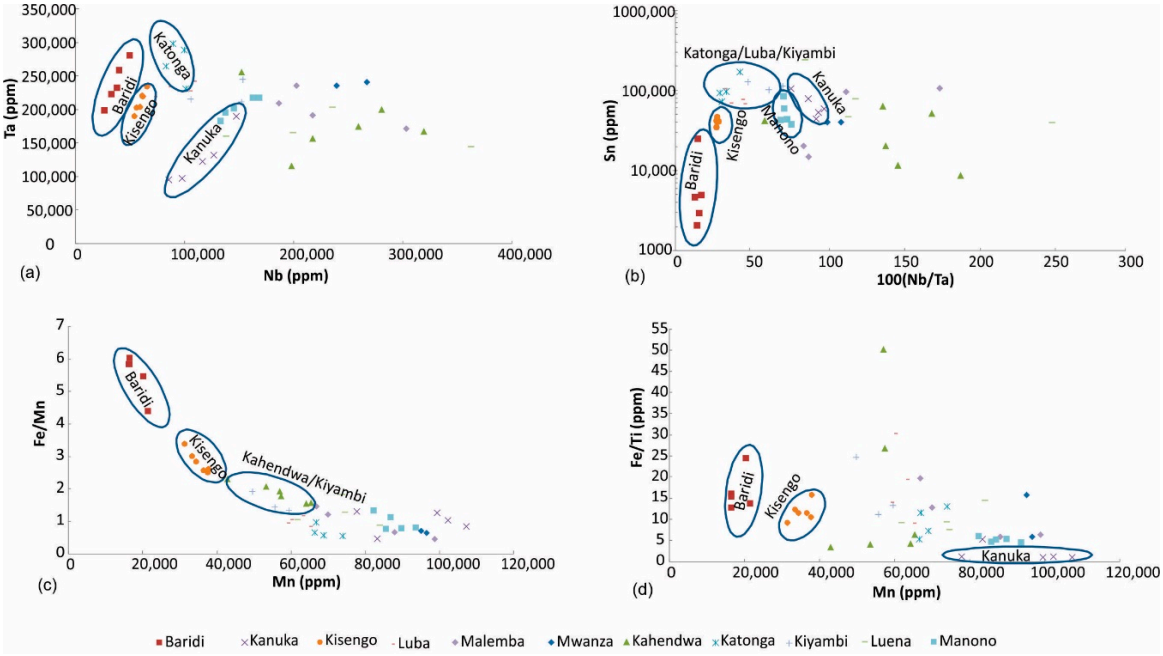

Figure 9. Discrimination of coltan ore samples based on (**a**) Nb and Ta, (**b**) 100 (Nb/Ta) vs. Sn, (**c**) Mn vs. Fe/Mn, (**d**) Mn vs. Fe/Ti.

Spider diagrams: These diagrams are used in geology to investigate elemental composition compared to a source such as Bulk Earth or Chondrite Meteorite. Concentrations of trace elements (Rb, Ba, Th, U, Ta, Nb, K, La, Ce, Sr, Nd, P, Zr, Ti, and Y) determined by FPXRF are plotted relative to Chondrite Meteorite [23] in the spider diagrams (Figure 10).

Coltan from most regions show a unique pattern in spider diagrams and this can be used as a fingerprinting tool. Manono and Luena samples show a very similar spider pattern and, therefore, the spider diagram of these regions should be used with other discrimination diagrams for effective discrimination.

In addition, elements used in these diagrams can be sorted out based on their chondrite-normalized concentrations to provide a powerful tool for fingerprinting coltan. The sorted arrays of elements are unique for coltan ore samples from each region (Table 7). The array of elements based on the normalized values are not the same. For example, the third highest element (based on the normalized value) in most deposits is U, whereas it is Th in Baridi and Kanuka.

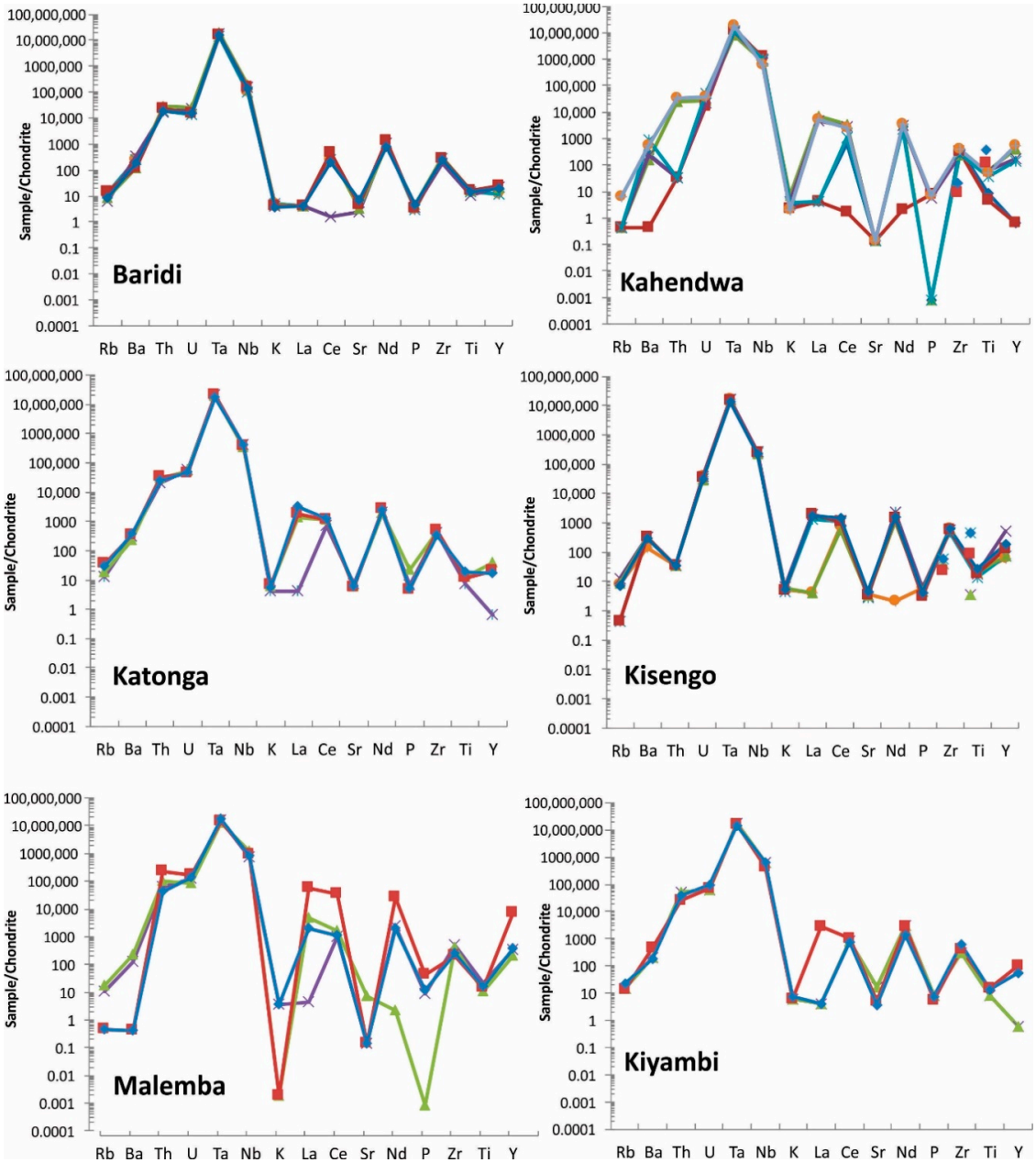

Figure 10. *Cont*.

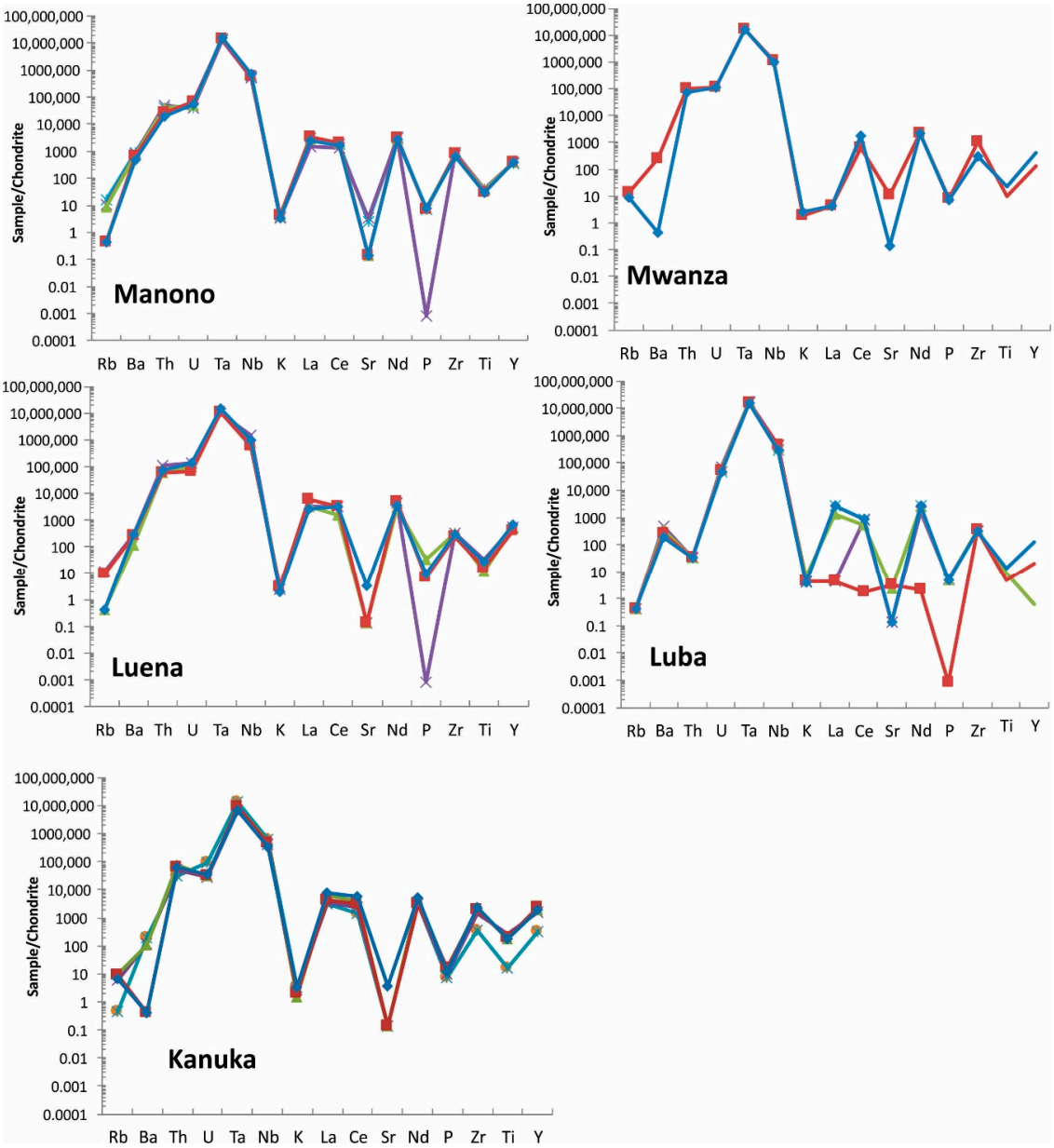

Figure 10. Spider diagram of coltan ore samples from all studied regions. Note that Manono and Luena samples show very similar pattern. For elements <LOD, half of detection limit is used for graphing purpose. Each sample is shown with a different color.

Table 7. Elements in chondrite-normalized coltan ore samples in order of increasing from left to right. Average values were used in the calculations. Based on chondrite-normalized values, Ta and Nb are the first and second highest elements, respectively, followed by other elements in each deposit.

Region	Elements														
Baridi	P	La	K	Sr	Rb	Ti	Y	Ba	Ce	Zr	Nd	U	Th	Nb	Ta
Kahendwa	Sr	Rb	P	K	Ti	Y	Zr	Ba	Ce	Nd	La	Th	U	Nb	Ta
Kanuka	Sr	K	Rb	P	Ba	Ti	Zr	Y	Ce	Nd	La	U	Th	Nb	Ta
Katonga	K	Sr	P	Ti	Y	Rb	Ba	Zr	Ce	La	Nd	Th	U	Nb	Ta
Kisengo	Sr	P	K	Rb	Ti	Th	Y	Ba	Zr	Ce	La	Nd	U	Nb	Ta
Kiyambi	K	P	Sr	Ti	Rb	Y	Ba	Zr	Ce	La	Nd	Th	U	Nb	Ta
Luba	Rb	Sr	P	K	Ti	Th	Y	Ba	Zr	Ce	La	Nd	U	Nb	Ta
Luena	Sr	K	Rb	P	Ti	Ba	Zr	Y	Ce	La	Nd	Th	U	Nb	Ta
Malemba	K	Sr	Rb	P	Ti	Ba	Zr	Y	Nd	Ce	La	Th	U	Nb	Ta
Manono	Sr	K	P	Rb	Ti	Y	Ba	Zr	Ce	La	Nd	Th	U	Nb	Ta
Mwanza	K	La	Sr	P	Rb	Ti	Ba	Y	Zr	Ce	Nd	Th	U	Nb	Ta

5. Conclusions

- HHXRF assay data shows that cassiterite and wolframite ores from all regions can be fingerprinted using various discrimination diagrams (Table 8). Although ore from some regions may be fingerprinted using a single discriminator (e.g., W + Th vs. Fe/Ti diagram for the Luena cassiterite ore), a combination of a few diagrams are often required to discriminate ore from most of the regions.
- Coltan ore samples from several regions can also be discriminated using major and trace elements of these samples. Baridi and Kisengo stand out chemically among the coltan ore samples. For other coltan regions, combinations of discrimination diagrams can be used to distinguish them. Coltan ore from some regions such as Luena, Malemba, and Mwanza have similar major element composition (Ta, Nb, Fe, Mn); however, distinctive spider diagram patterns can be used as a fingerprinting tool. In addition, Chondrite-normalized elemental arrays reflect characteristic trace element distributions in coltan ore from various regions, which in turn is related to the specific ore and mineral chemistry in each region.

This study demonstrates that a handheld XRF has the potential to provide immediate screening and indication of the origin of the mineral, and may provide an additional tool for rapidly determining provenance of some conflict minerals. However, this test is based on limited samples; with the speed of analysis that handheld XRF offers, more samples from other parts of the world can be analyzed to create a global library/data set for further detailed fingerprinting. Such a library can be used to fingerprint conflict mineral in-situ and in real time. Such a discriminating handheld analyzer would be invaluable for various industries and custom offices around the world.

Table 8. Discriminators that are used for fingerprinting conflict minerals.

Ore Type	Discriminator	Composite Factors	Discriminated Region
Cassiterite	Sn-W-(Ta + Nb) triangular	Sn/10, 20 W, 20(Ta + Nb)	Overall cassiterite composition of all regions
	Sn vs. (Fe/Ti)	Sn vs. 100(Fe/Ti)	Malemba, Mwanza, Commir, Luena, Busanga
	Ti vs (Ti/Nb + Ta)	Ti vs. 100(Ti/Nb + Ta)	Mitwaba, Busanga
	W + Th vs. Fe/Ti	Log(W + Th) vs. 100(Fe/Ti)	Luena
	Y + Th vs. Nb+Ta	Y + Th vs. Log(Nb + Ta)	Busanga, Commir, Manono, Kanuka
	W + Th vs. Ti/(Ta + Nb)	Log(W + Th) vs. Log(100Ti/(Ta + Nb))	Mitwaba, Kindu, Luena
	Ta/Nb vs. Ti/(Ta + Nb)	100Ta/Nb vs. Log(100Ti/(Ta + Nb))	Busanga, Mitwaba, Malemba, Mwanza
Wolframite	Sn-W-(Ta + Nb) triangular	Sn, W, (Ta + Nb)	Overall wolframite composition of all regions
	W-Fe-Mn	W, 10Fe, 10Mn	Katonga, Luena, Manono
	Fe vs. Mn	Fe, Mn	Katonga, Luena, Manono
	W vs. Sn	W, Sn	Katonga, Luena, Manono
	W vs. Th	W, Th	Katonga, Luena, Manono
	Sn vs. Th	Sn, Th	Katonga, Luena, Manono
	W vs. Zr	W, Zr	Katonga, Luena, Manono
	W/Sn vs. Zr	Log(W/Sn), Log(Zr)	Katonga, Luena, Manono
Coltan	Nb vs. Ta	Nb, Ta	Baridi, Kisengo, Katonga, Kanuka (?)
	Nb/Ta vs. Sn	100 Nb/Ta, LogSn	Baridi, Kisengo, Manono, Kanuka, Katonga/Luba/Kiyambi
	Mn vs. Fe/Mn	Mn, Fe/Mn	Baridi, Kisengo, Kahendwa/Kiyambi
	Mn vs. Fe/Ti	Mn, Fe/Mn	Baridi, Kisengo, Kanuka
	Spider diagrams	Rb, Ba, Th, U, Ta, Nb, K, La, Ce, Sr, Nd, P, Zr, Ti, Y all divided by same elements in Chondrite Meteorite	Most regions have unique spider pattern.

Funding: This research was funded by ThermoFisher Scientific.

Acknowledgments: Samples for this case study were provided by MMR (Mining Mineral Resources), Democratic Republic of Congo and I am very grateful for logistics and having access to MMR lab. Also, Ingo Steinhage

(United Spectrometer Technologies) and John Kande (Ets United Technologies & Ets United Scientific) are thanked for their field and logistic help. ThermoFisher Scientific is greatly appreciated for providing the handheld analyzer. The manuscript benefited from constructive comments made by three anonymous reviewers. Special thanks to Anderson for her edits and comments.

Conflicts of Interest: The authors declare no conflict of interest.

References

1. Melcher, F.; Sitnikova, M.A.; Graupner, T.; Martin, N.; Oberthür, T.; Henjes-Kunst, F.; Gäbler, E.; Gerdes, A.; Brätz, H.; Davis, D.W.; et al. Fingerprinting of conflict minerals: Columbite-tantalite ("coltan") ores. *SGA News* **2008**, *23*, 7–14.
2. Conrey, R.M.; Goodman-Elgar, M.; Bettencourt, N.; Seyfarth, A.; Van Hoose, A.; Wolff, J.A. Calibration of a portable X-ray fluorescence spectrometer in the analysis of archaeological samples using influence coefficients. *Geochem. Explor. Environ. Anal.* **2012**, *14*, 291–301. [CrossRef]
3. Arne, D.C.; Mackie, R.A.; Jones, S.A. The use of property-scale portable X-ray fluorescence data in gold exploration: Advantages and limitations. *Geochem. Explor. Environ. Anal.* **2014**, *14*, 233–244. [CrossRef]
4. Cheng, Q. Vertical distribution of elements in regolith over mineral deposits and implications for mapping geochemical weak anomalies in covered areas. *Geochem. Explor. Environ. Anal.* **2014**, *14*, 277–289. [CrossRef]
5. Gazley, M.F.; Tutt, C.M.; Brisbout, L.I.; Fisher, L.A.; Duclaux, G. Application of portable X-ray fluorescence analysis to characterize dolerite dykes at the Plutonic Gold Mine, Western Australia. *Geochem. Explor. Environ. Anal.* **2014**, *14*, 223–231. [CrossRef]
6. Lemiere, B.; Laperche, V.; Haouche, L.; Auger, P. Portable XRF and wet materials: Application to dredged contaminated sediments from waterways. *Geochem. Explor. Environ. Anal.* **2014**, *14*, 257–264. [CrossRef]
7. Quiniou, T.; Laperche, V. An assessment of field-portable X-ray fluorescence analysis for nickel and iron in laterite ore (New Caledonia). *Geochem. Explor. Environ. Anal.* **2014**, *14*, 245–255. [CrossRef]
8. Simandl, G.J.; Paradis, S.; Stone, R.S.; Fajber, R.; Kressall, R.D.; Grattan, K.; Crozier, J.; Simandl, L.J. Applicability of handheld X-Ray fluorescence spectrometry in the exploration and development of carbonatite-related niobium deposits: A case study of the Aley Carbonatite, British Columbia, Canada. *Geochem. Explor. Environ. Anal.* **2014**, *14*, 211–221. [CrossRef]
9. Vaillant, M.L.; Barnes, S.J.; Fisher, L.; Fiorentini, M.L.; Caruso, S. Use and calibration of portable X-Ray fluorescence analysers: Application to lithogeochemical exploration for komatiite-hosted nickel sulphide deposits. *Geochem. Explor. Environ. Anal.* **2014**, *14*, 199–209. [CrossRef]
10. Yuan, Z.; Cheng, Q.; Xia, Q.; Yao, L.; Chen, Z.; Zuo, R.; Xu, D. Spatial patterns of geochemical elements measured on rock surfaces by portable X-ray fluorescence: Application to hand specimens and rock outcrops. *Geochem. Explor. Environ. Anal.* **2014**, *14*, 265–276. [CrossRef]
11. Hunt, A.M.W.; Speakman, R.J. Portable XRF analysis of archaeological sediments and ceramics. *J. Archaeol. Sci.* **2015**, *53*, 626–638. [CrossRef]
12. Kuster, D. Granitoid-hosted Ta mineralization in the Arabian-Nubian Shield: Ore deposit types, tectonometallogenetic setting and petrogenetic framework. *Ore Geol. Rev.* **2009**, *35*, 68–86. [CrossRef]
13. Shaw, R.; Goodenough, K.; Gunn, G.; Brown, T.; Rayner, D. Niobium and tantalum. *Br. Geol. Surv. Publ.* **2011**, *2011*, 27.
14. Nasraoui, M.; Bilal, E. Pyrochlore from the Lueshe carbonatite complex (Democratic Republic of Congo): A geochemical record of different alteration stages. *J. Asian Earth Sci.* **2000**, *18*, 237–251. [CrossRef]
15. Tack, L.; Wingate, M.T.D.; De Waele, B.; Meert, J.; Belousova, E.; Griffin, B.; Tahon, A.; Fernandez-Alonso, M. The 1375 Ma Kibaran event' in Central Africa: Prominent emplacement of bimodal magmatism under extensional regime. *Precambrian Res.* **2010**, *180*, 63–84. [CrossRef]
16. Hulsbosch, N.; Hertogen, J.; Dewaele, S.; Andre, L.; Muche, P. Petrographic and mineralogical characterization of fractionated pegmatites culminating in the Nb-Ta-Sn pegmatites of the Gatumba area (western Rwanda). *Geol. Belg.* **2013**, *16*, 105–117.
17. Dewaele, S.; Fernandez-Alonso, M.; Tack, L. Cassiterite and columbo-tantalite (Coltan) mineralisation in the Proterozoic rocks of the northern part of the Kibara orogen (Central Africa): Preliminary results. *Bull. Scéanc. Acad. R. Sci. Outre-Mer* **2008**, *54*, 341–357.

18. Romer, R.L.; Lehmann, B. U-Pb Columbite Age of Neoproterozoic Ta-Nb Mineralisation in Burundi. *Econ. Geol.* **1995**, *90*, 2303–2309. [CrossRef]
19. Somarin, A.K.; Ashley, P. Hydrothermal alteration and mineralization of the Glen Eden Mo-W-Sn deposit: A leucogranite-related hydrothermal system, Southern New England Orogen, NSW, Australia. *Miner. Deposita* **2004**, *39*, 282–300.
20. Gäbler, H.; Melcher, F.; Graupner, T.; Bahr, A.; Sitnikova, M.A.; Henjes-Kunst, F.; Oberthür, T.; Brätz, H.; Gerdes, A. Speeding up the analytical workflow for coltan fingerprinting by an integrated mineral liberation analysis/LA-ICP-MS approach. *Geostand. Geoanalytical Res.* **2011**, *35*, 431–448. [CrossRef]
21. Harka, R.; Remus, J.J.; East, L.J.; Harmon, R.S.; Wise, M.; Tansi, B.M.; Shughrue, K.M.; Dunsin, K.; Liu, C. Geographical analysis of "conflict minerals" utilizing laser-induced breakdown spectroscopy. *Spectrochim. Acta Part B At. Spectrosc.* **2012**, *74*, 131–136. [CrossRef]
22. Arnaud, C.H. Fingerprinting conflict minerals: Spectroscopic method could help identify mineral origins. *Chem. Engin. News* **2012**, *90*, 36–37.
23. Su, S.S.; McDonough, W.F. Chemical and isotopic systematics of oceanic basalts: Implications for mantle composition and processes. In *Magmatism in Ocean Basins*; Saunders, A.D., Norry, M.J., Eds.; Geological Society, London, Special Publications: London, UK, 1989; pp. 313–345.